Crimson Publishers
Wings to the Research

Research Article

Experimental Study on Compression Deformation Characteristics of Soil-rock Mixture under Saturated Pore Water Pressure

Tongsuo Guo[1,2], Qingxiang Cai[1], Wei Zhou[1]*, Xiaohua Ding[1] and Xuyang Shi[1]

[1]School of Mines, China

[2]Inner Mongolia Baoli Coal Co, China

ISSN: 2639-0574

***[1]Corresponding author:** Wei Zhou, School of Mines, China

Submission: November 13, 2019

Published: November 18, 2019

Volume 3 - Issue 5

How to cite this article: Tongsuo G, Qingxiang C, Wei Z, Xiaohua D, Xuyang S. Experimental Study on Compression Deformation Characteristics of Soil-rock Mixture under Saturated Pore Water Pressure. Adv Civil Eng Tech. 3(5). ACET.000573.2019. DOI: 10.31031/ACET.2019.03.000573

Abstract

The dump of open-pit coal mine is reconstructed by loose soil-rock mixture under the action of gravity, dynamic load of transportation equipment, blasting vibration and so on. Due to the saturated state of rainfall or groundwater flow, if the drainage is not timely, excess pore water pressure will occur in the remolded slope of the dump, and the sliding resistance of the slope will be reduced. In order to simulate the working condition, the compression-seepage coupling characteristics of soil-rock mixtures under saturated pore water pressure were tested under three factors: particle size, rock content and loading rate. The experimental results show that the soil-rock particles in the area affected by pressure change in vertical direction step by step, and the displacement field formed by soil-rock particles is similar to bowl shape. With the increase of sand particle size, the influence range of displacement field of soil-rock mixtures decreases gradually, and the range of displacement field of soil-rock mixtures synthesized with 0.1-0.5mm sand particle size is the largest. With the increase of rock content, the influence range of displacement field of soil-rock mixtures becomes smaller. The loading rate has little effect on the displacement field of soil-rock mixture.

Keywords: Open-pit coal mine; Soil-rock mixture; Pore water pressure; Seepage flow; Displacement field

Introduction

The production activity of open pit coal mine is essentially to construct excavation space in the upper part of coal seam, and the stripped loose soil and gravel are mixed to form loose soil and stone remolding body of dump. Under the action of water, stress and other factors, bulk soil-rock mixture cements to a certain extent. With the development of time and the change of factors affecting cementation, the cementation degree of bulk soil-rock mixture changes continuously. Macroscopic manifestation is the change of physical and mechanical properties and hydraulic characteristics. This process is called the remolding process of soil-rock mixture. The open-pit dump is formed by the aggregation of loose soil-rock under the action of gravity, the dynamic load of transportation equipment and blasting vibration. Accurately understanding the law of deformation and the evolution of the soil-rock aggregate during remodeling is crucial for evaluating the stability of the dump slope. However, with the dumping site's large volume, the complex structure of the soil-rock aggregate, and the long sedimentation time, it is difficult to monitor the reconstruction and deformation of the soil-rock aggregate through field tests. The indoor similar simulation test has been widely used in many engineering practices as an intuitive study of geotechnical physics characteristics. Therefore, this method will be used to study the reconstruction and deformation of the soil-rock aggregate. Meanwhile, it will provide an important experimental basis for the overall stability evaluation of the open-pit dumps [1].

In order to facilitate the preparation and research of the sample, and take into account the principle of controlling variables, the soil and rock mass in the sample of soil-rock mixture prepared in this experiment are directly selected from the clay and sandstone which are mainly discarded in the dump of Haerwusu Open-pit Coal Mine, China, as shown in Figure 1. In 1973, Chandler [2] found that when the sample contains large stones, the strength of the sample would be greatly improved, but the increased strength did not represent the true strength of the stone-containing samples. In response to this phenomenon, many domestic and foreign scholars have begun several studies and proposed the concept of the soil-rock aggregate.

Figure 1: The dump of Haerwusu open-pit coal mine.

In the study of the permeability of the soil-rock aggregate, the permeability coefficient of the aggregate of both the earth and rock was proportional to the pore ratios, and these were approximately related to the non-evenness [3]; researchers identified the influence priority of particle size, void ratio and particle shape on the permeability of the soil-rock aggregate through indoor experiments [4-6]. In terms of its mechanical properties, the shear strength and internal friction angle of the soil-rock aggregate decreased with the increase in the moisture capacity through internal direct shear tests [7]. Vieira et al. [8] identified the level of influence of the factors affecting the shear strength of the soil-rock aggregate through large shear test; the order of these were the size of the stone, the stone content, and the block arrangement. It was found that there were many similarities between the typical stress-strain curves of the soil-rock aggregate and the rock by studying the strength of the soil-rock aggregate with the fractal theory [9]. The fractal dimension of the particle size had a great influence on the strength of the soil-rock aggregate. The best soil-rock aggregate was the mixture with a one-dimensional fractal; Qiang et al. [10] obtained the morphology, location and content of the soil-rock aggregate and based on these samples. They also analyzed the relationship between the stone content and the mechanical properties of the soil-rock aggregate through digital image analysis and processing technology. Li et al. [11] studied the relationship between the features of the soil-rock aggregate and stress-strain under the uniaxial theory by applying fractal geometry theory.

In the study of the deformation and failure in soil-rock aggregates, Wang et al. [12] studied the significant characteristics of the deformation and failure of the soil-rock aggregate through the CT test and divided the causes of damage to the aggregate into three grades: the interface cracks; the generation, expansion, and interlocking of soil cracks until destruction; and weak rock damage. Sun et al. [13] improved CT scanning method to identify cracks and damage and wrote a program to analyze the internal changes of the soil-rock aggregate under uniaxial compression. The three-dimensional reconstruction model of soil-rock aggregate failure and damage was established. The destruction of the soil-rock aggregate was related to the stone-content rate and similar to the stone-content rate of the damage. Zhou et al. [14] regarded the soil-rock aggregate as an ideal binary mixture and applied homogenization theory to explore the stress-strain relationship of the soil-rock aggregate. Further, he ensured that the results compared well with the data obtained from the triaxial test, and as a result, homogenization theory can be used to represent the stress-strain relationship of the soil-rock aggregate. Yuan et al. [15] compressed the samples and used X-ray scanning and analyzed the migration law of the earth and rock during the internal deformation and destruction of the aggregate; they found that the damage to the sample expands from the concentrated stone to the earth interface until it was destroyed.

The content of the above research mainly focused on the geometric, physical and mechanical properties, the deformation failure mechanism and the establishment of the constitutive relationship of the soil-rock aggregate, but most of them did not include the influence of the loading rate and the soil-rock aggregate on the remodeling deformation. The main purpose of the model test in this paper is to reproduce the migration process of the internal soil-rock aggregate in the open-pit dump. During the test, it was necessary to collect data on the development process and morphology of the soil, stone and soil-stone mixture under vertical pressure. To satisfy the above test requirements and obtain the desired results, the transparent soil-rock aggregate and the supporting test equipment for the strip mine pump were developed independently, and then the effect of different compression affected areas (pressure plate impact region and extended influence region), the particle size, stone arrangement and loading rate on the remodeling deformation of the soil-rock aggregate were studied.

Materials and Methods

Experimental moulds

Considering the large size of the open-pump and the limited geometrical dimensions of the model, and in order to ensure the accuracy of the test, the geometric similarity ratio was determined to be 100, so the internal dimensions (thick × lateral width × height) of the experimental models were determined to be 0.15m × 0.15m × 0.19m. To improve the accuracy of the data, the test was carried out in real time using a high-precision digital camera, which required that the test moulds be transparent. Acrylic sheets were selected for the experimental molds due to their high strength, toughness, easy processing, and good designability. To ensure the strength of the moulds without affecting the transparency and the shooting effect, the thickness of the acrylic sheet was set to 20mm. The structural dimensions of the mould are shown in Figure 2.

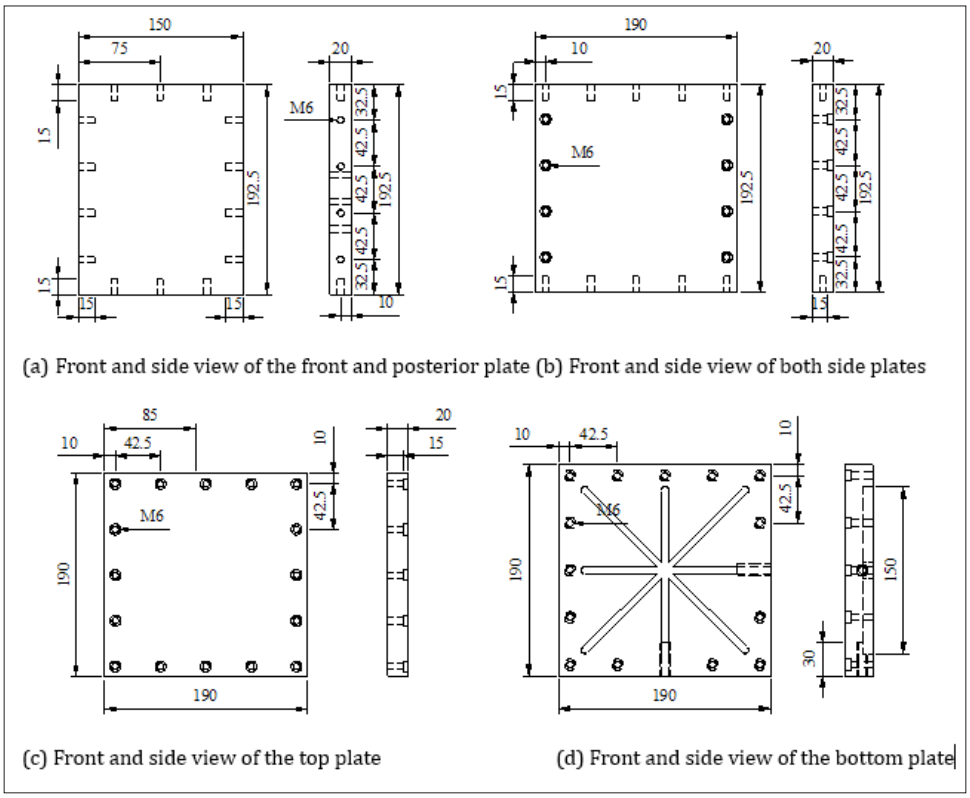

Figure 2: The dimensions of the mould (Unit: mm).

Because the mould frame needs to withstand a large expansion force during the test, in order to ensure the integrity of the mould, it needs to be reinforced with an external frame. The frame was cut with 8 aluminum rods of 10mm thickness. The actual figure is shown in Figure 3.

Figure 3: External frame.

Test loading devices

This experiment adopted a uniaxial compression experimental system of transparent similar materials (Figure 4). The system can be controlled through a computer, which can control the pressure loading or control the displacement loading and can monitor the head displacement and the load data in real time. The loading platform was square, which was convenient for the installation and disassembly of the moulds, and the surroundings were unobstructed, which was convenient for the use of the photogrammetric system.

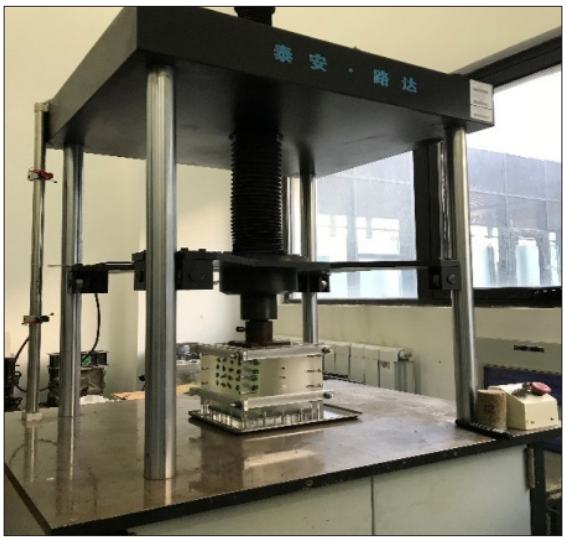

Figure 4: Uniaxial compression experimental system for transparent similar materials.

Image collection system

The speckle surface was laid on the observation surface of the model. After the application of vertical pressure, the position of the speckle was observed through the image acquisition system and then used to analyze the internal migration and the law of deformation of the soil-rock aggregate. The image acquisition system consists of a digital camera (EOS60D Canon Inc), a tripod, two lights, and a computer, as shown in Figure 5. The analysis and processing of the image data was performed by the Photo Infor image analysis software and the Post Viewer post-processing software. Photo Infor could be used to analyze the deformation of images, such as scatter, crack, cleft and shear band deformation, and then, Post-Viewer would be used to extract images and analyze the data.

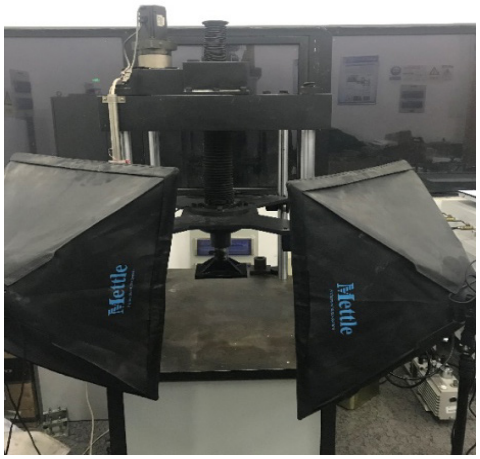

Figure 5: Image collection system.

Penetration test

The worst period of stability of open pit dump is when the soil-rock mixture of dump is saturated due to rainfall or groundwater flow. At this time, the excess pore water pressure caused by poor drainage of the soil-rock mixture reduces the anti-sliding force of the slope. In order to simulate this working condition, the sample is saturated or nearly saturated by suction and penetration test before continuous loading compression test. The specific steps are as follows:

A. Put the sample into the saturator of triaxial apparatus, and place filter paper and permeable stone at the upper and lower ends respectively. Then tighten the knob at one end of the tie rod to ensure the stability of the shell.

B. Put the saturator of the fixed sample into the vacuum cylinder, smear Vaseline between the vacuum cylinder and the cylinder head, and tighten the cap. Connect the pumping unit with the vacuum cylinder and start the pumping unit. When the vacuum pressure gauge is close to an atmospheric pressure value, the pumping lasts for 2 hours. After that, turn on the switch of the connecting water tank and let the water enter the vacuum cylinder. When the water level reaches the position of fully submerged saturator, turn off the switch and stop filling water, and keep the vacuum pumping state for 48 hours, as shown in Figure 6.

Figure 6: Vacuum saturation.

C. The saturated sample is taken out from the vacuum cylinder and saturator, and six filter strips with a width of one centimeter are affixed to the outer wall of the sample longitudinally and equidistantly to ensure that the filter strips do not contact the top and bottom of the sample, thus accelerating the moisture movement in the sample.

D. The GDS (Geotechnical Test Bench of Euro-American Geotechnical Instruments and Equipment China Ltd.) pressure chamber platform and pipelines will be exhausted, and then the samples will be wrapped with latex film and fixed on the pressure chamber platform. After contacting and fixing the sample with the upper and lower water heads, the sample is exhausted by suction ball and controller to ensure that there are no obvious bubbles between the latex film and the outer wall of the sample.

E. Fix the pressure chamber tightly on the platform through the knob, open the water valve and pump, fill the pressure chamber slowly, and seal well, so that there are no obvious bubbles in the pressure chamber. By manually rotating the cap, the contacts in the pressure chamber are contacted with the Back Pressure head controller on the upper part of the sample, resulting in a force of about 0.05kN, which enables the upper and lower heads of the sample to be close to the sample during the seepage process.

F. Through the GDS control software on the computer, the seepage module is selected, Cell Pressure is adjusted to 150kPa, Back Pressure to 130kPa and Base Pressure to 100kPa, so that the normal head permeation test with osmotic pressure of 30kPa is carried out.

G. The permeability coefficient of the sample can be obtained when the volume change curve is stable, and the velocity of water inflow is the same as that of drainage. It usually takes 12 to 24 hours from the beginning of seepage to the stability.

Test methods and procedures

The open-pit dump was made up of soil, stone and the mixture of these two materials, which were remodeled under the action of gravity acting on the sand and external loads, such as mining trucks and earthquakes. There were many factors that can affect the remodeling process, such as the size and content of soil and stone and the size of the load. This paper focused on the deformation process and morphological characteristics of the soil-rock aggregate during the open-pit dump remodeling process. The three influencing factors of sand particle size, stone content and loading rate were selected. The designed test plans are shown in Table 1.

Table 1: Test plans.

Test Number	Silica Sand Particle Size	Stone Arrangement	Loading Rate (mm/min)
1-1	Fine sand	3×3	3
1-2	Mixed sand	3×3	3
1-3	Coarse sand	3×3	3
2-1	Fine sand	3×3	5
2-2	Mixed sand	3×3	5
2-3	Coarse sand	3×3	5
3-1	Fine sand	4×4	3
3-2	Mixed sand	4×4	3
3-3	Coarse sand	4×4	3
4-1	Fine sand	4×4	5
4-2	Mixed sand	4×4	5
4-3	Coarse sand	4×4	5

The particle size of fine sand in the above table were from 0.1 to 0.5mm, the size of coarse sand was from 0.5 to 1.0mm, and the mixed sand consisted of a mixture of coarse and fine sand with a mass ratio of 1:1. The 3×3 stone arrangement contained 9 stones that were arranged in a 3×3 network format, and the 4×4 arrangement contained 9 stones arranged in a 4×4 network format.

Experimental procedures:

a. The fused silica sand and the stones were cleaned and dried and disposed with the transparent sand.

b. The test mould was assembled, the rear panel was filled with transparent sand, a square permeable stone was placed in both in the upper and lower parts, the bottom of the test mould was filled with transparent sand using a spoon until it was a quarter of the way full, and finally, the mould was filled in a vacuum pump to extract air in order to maintain the transparency of the model;

c. After the end of the pumping, we continued to fill the model with transparent sand; when the mould was half full, we pumped again; finally, we laid the speckle surface and stones as shown in Figure 7.

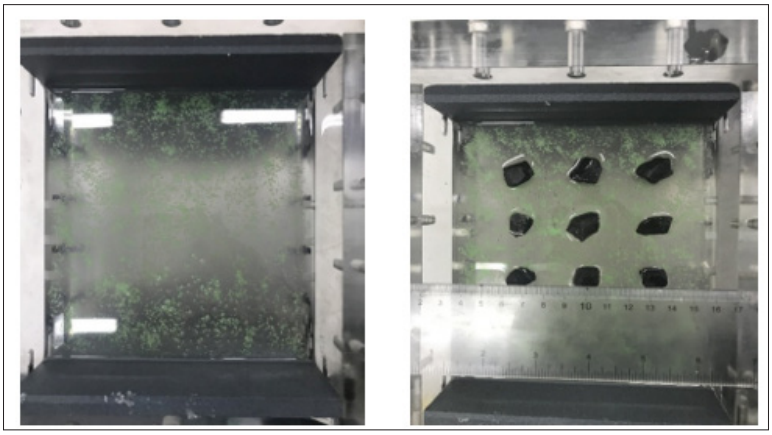

Figure 7: Laying the speckle surface and stones in the moulds.

d. After laying the speckle and stones onto the surface, transparent sand was poured onto it until the whole mould was filled. The pouring process was also performed layer by layer, and each layer needed to be pumped after pouring;

e. We sealed the rear panel, set the mould up and left it to stand for a while, after which we stabilized it, placed it on the test bench for uniaxial compression of transparent similar material and removed the upper panel and the permeable stone. We then directly placed the model in the center of the test bench;

f. A digital camera was set up, we adjusted the height of the camera in order to be flush with the center of the model, and we placed the camera in front of the model and adjusted the focal length of camera in order to obtain the optimal imaging distance. We then placed two lights on both sides of the camera to illuminate the light source;

g. We lowered the pressure plate until it touched the model and the computer showed a strong contact stop, at which point we zeroed the press; finally, we set the frequency of the camera to 2 frames/sec;

h. At the same time, the switch was pressed to make use of the transparent-similar material with the uniaxial compression experimental system and the digital camera at the same time, until the end of the test when we stopped collecting images, unloaded the pressure, and cleaned the mould.

Study of the Law of the Soil-rock Aggregate during the Reconstruction

During remodeling of the soil-rock aggregate under the uniaxial loading, the soil moved in a specific direction under the vertical pressure by the pressure plate. With the continuous vertical pressure, normal stress was generated between the soils, and this caused displacement. Then, the Photo-Infor and Post-Viewer software were used to process the experimental images, and the migration of the soil-rock aggregate during the remodeling process was analyzed. According to the results of this test, the soil-rock aggregate can be divided into the pressure plate zone and the extended zone (Figure 8).

Law of transparent soil migration affected by the pressure plate

Since the output of the pressure head of the transparent-similar material was under uniaxial compression testing, the law of transparent soil migration in the area affected by the pressure plate was also complicated. The images collected from samples with fused silica sand particle sizes ranging from 0.1 to 0.5mm and 0.5 to 1.0mm mixed with a mass ratio of 1:1, the arrangement of stone within a 4×4 grid, and the loading rate of 3 mm/min were used to analyze the transport of transparent soil particles. The migration map of the transparent soil affected by the compression plate is shown in Figure 9.

From Figure 9, we can conclude that in the regions affected by the pressure plate, there was a transparent soil migration tendency. In the region directly under the pressure plate, the transparent soil was subjected to vertical force, and the soil was moved directly downward, which was migration in the direction of pressurization. This meant that the transparent soil in the area directly under the pressure plate was in the shape of the compression deformation, and the closer soil was to the pressure plate, the smaller the compression. The amount of compression was inversely proportional to the distance from the pressure plate.

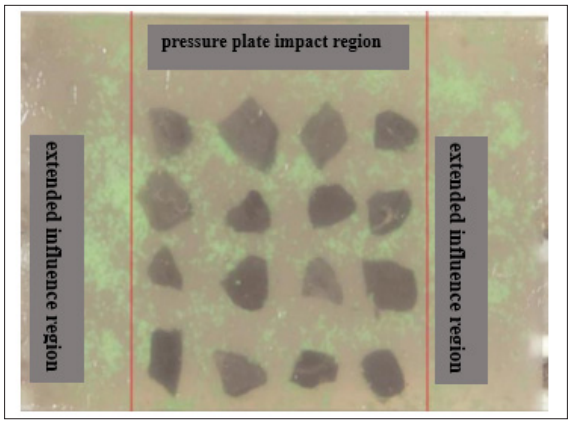

Figure 8: Affected regions.

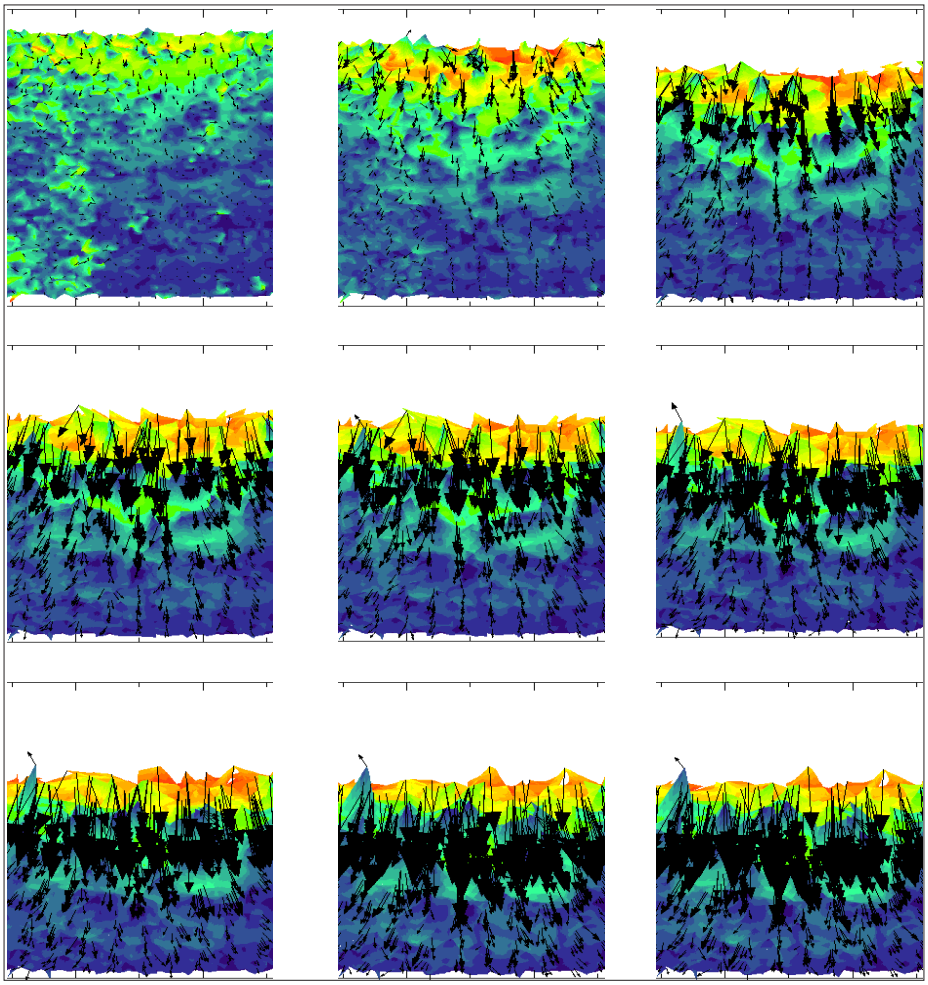

Figure 9: The migration map of the transparent soil affected by the compression plate.

On both sides of the pressure plate, the soil was subjected to lateral pressure from the pressure plate, and the soil moved downwards or in the horizontal direction. The closer the soil particles were to the left and right edges of the pressure plate, the greater the angle between the pressurization direction and the vertical. The law of soil migration affected by the pressure plate in the area changed stepwise in the vertical direction.

The Law of migration of soil in the affected regions

During the reconstruction process under vertical pressure, the soil particles on the left and right sides of the pressure plate also experienced deformation and reconstruction due to the extrusion of surrounding soil particles. The migration of soil in the affected regions is shown in Figure 10.

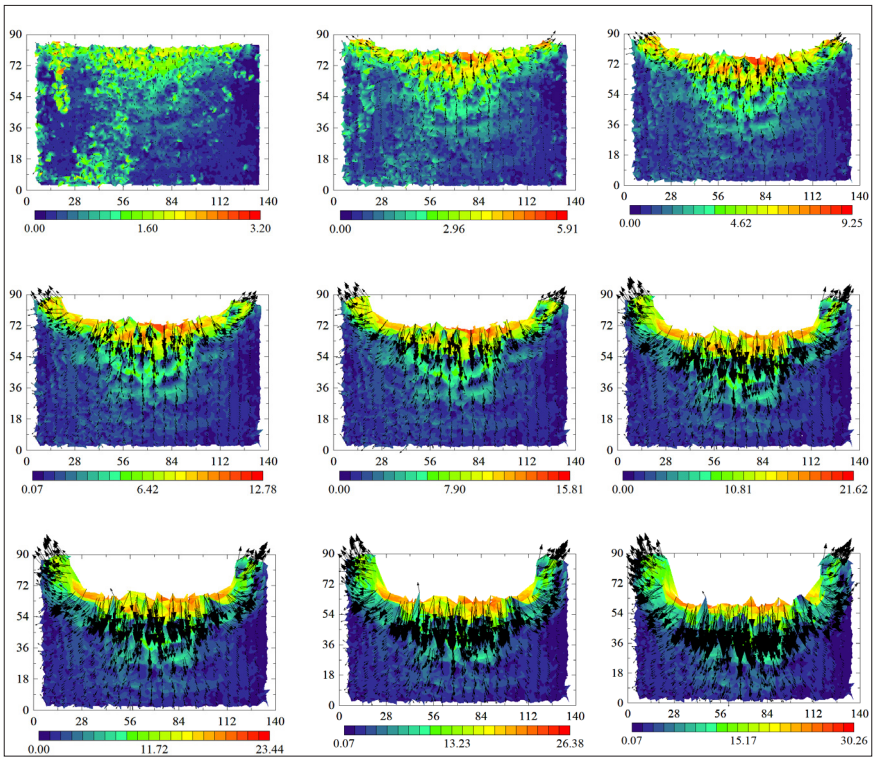

Figure 10: The migration of soil in the affected regions.

From Figure 10, we could conclude that the migration of soil particles was divided into two parts in the extended area. One was that the two sides of the soil particles under the pressure plate were pushed by the aggregated soil particles, so the angle between the direction of soil migration and the vertical trend was less than 90°, and the angle would decrease as the distance from the center of the pressure plate increased. The second was that the soil particles in the extended influence regions were initially pushed horizontally from the pressure plate on both sides of the edge of the pressure plate and the soil particles. The squeezing action moved in the horizontal direction, and then, with the increase in the compression of the pressure plate, the soil body was moved upward obliquely, and the movement angle gradually increased under the pushing action and the boundary binding force of the moulds.

Analysis of the Factors Affecting Reconstruction and Deformation of the Earth and Rock Aggregate

Particle size of soil affected the reconstruction of soil-rock aggregate

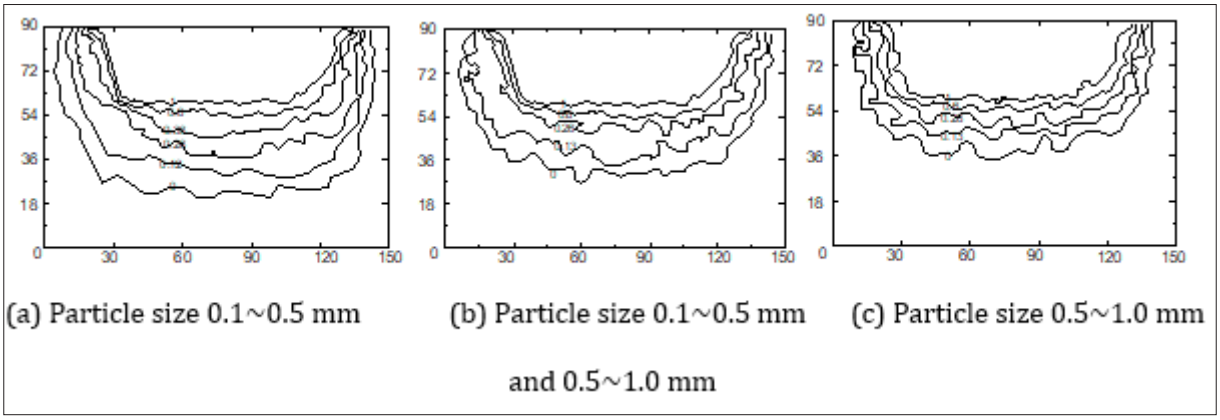

Figure 11: The contour map of migration of different particle size.

The particle size of the soil was one of the important engineering geological properties of the soil-rock aggregate, and it was also an important factor affecting the change in the migration field. Under the premise of ensuring that other influencing factors were unchanged, the particle size of the soil was controlled to simulate the influence of the particle size of different soils on the displacement field during the remodeling process of the soil-rock mixture under vertical pressure. The sample stones were arranged in a 4×4 mode,

the loading rate was 3mm/min, and the particle size of the fused silica sand ranged from 0.1~0.5mm, 0.5~1.0mm, 0.1~0.5mm and 0.5~1.0mm. The contour map of the final migration shape of the soil-rock aggregate with a proportion of 1:1 is shown in Figure 11.

As shown in Figure 11, the particle size of the soil had an important influence on the range of the migration field of the soil-rock aggregate and had little effect on the deformation mode. In the sphere of influence, with the increase in the particle size of the soil particles, the range of influence of the soil particles showed little change in the position adjacent to the pressure plate, and a displacement field of approximately 30mm formed along the side of the plate's surface. The range of influence of the displacement field formed by the soil particles in the side region is largely unchanged. The influence range of the displacement field of three different soil particle sizes was between 0 and 30mm and 120 and 150mm in the X direction and between 63 and 90mm in the Y direction, and the trend of the change was stable. However, under the pressure plate, as the particle size of the soil increased, the influence range of the displacement field of the soil-rock aggregate decreased gradually.

In the steady state, the displacement fields of the soil-rock aggregate of the three groups of different soil particle sizes demonstrated a "groove type" distribution. When the particle size of the soil ranged from 0.1 to 0.5mm, the displacement field of the soil-rock aggregate had a maximum influence range of 18 to 90mm in the Y direction. When the particle size of soil is 0.1-0.5 mm and 0.5-1.0 mm mixed, the displacement field ranged from 27 to 90mm in the Y direction; when the particle size of the soil ranged from 0.5 to 1.0mm, the maximum influence range of the displacement field was 36 to 90mm in the Y direction. In addition, for the soil particles at the same position, the migration gradually decreased along the Y direction; as the particle size of the soil increased, the vertical displacement of the soil particles at the same position also slowed.

It can be seen that in the case with the same arrangement and loading rate of the stones, as the particle size of the soil increased, the range of influence of the displacement field of the soil-rock aggregate generated decreased when the pressure plate moved at an even speed. In the soil-rock aggregate, when the particle size of the soil was smaller, the effective stress was also smaller, and a large-scale displacement field was easily generated under the same vertical stress. The opposite was not true.

Influences of stone arrangement on the soil-rock aggregate

In this test, the particle size of the soil ranged from 0.1 to 0.5mm, the loading rate was 5mm/min, and the arrangement of the stones was 3×3 and 4×4. The deformation cloud diagrams of the soil-rock aggregate under different stone arrangement modes are shown in Figure 12. It can be seen from Figure 12 that under two different stone arrangements, the displacement field of the soil-rock aggregate has the same pattern, and all belong to the "groove type" displacement field, but the range of influence of the displacement field show certain differences. The displacement field of the soil-rock aggregate under two different types of stone arrangements are shown in Figure 13.

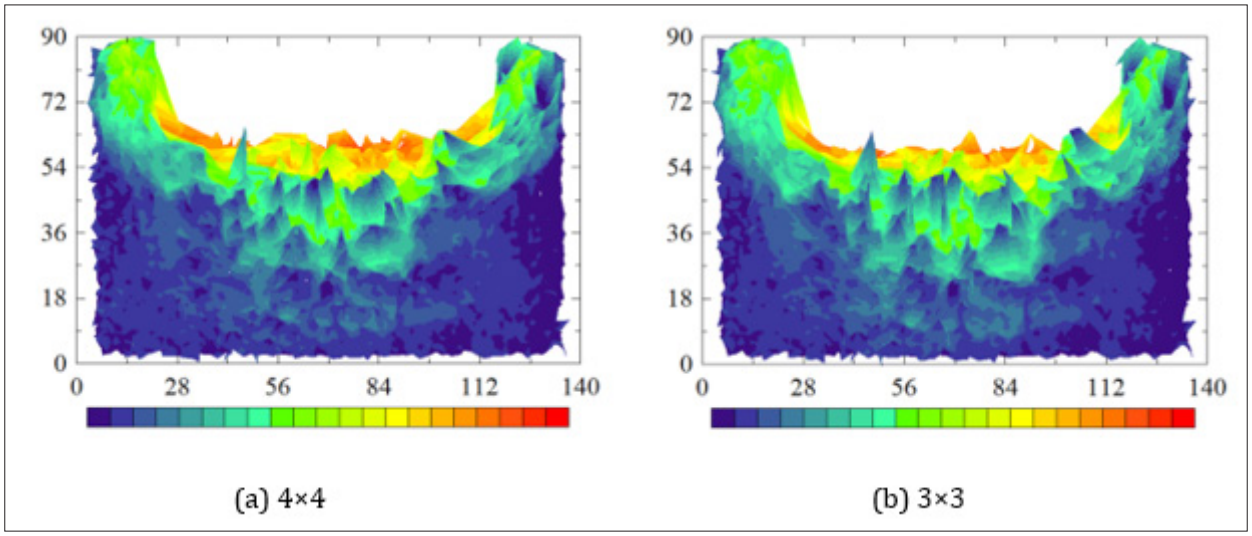

Figure 12: Cloud diagrams of different stone arrangements.

It can be seen from Figure 13 that as the number of stones increased, the displacement field showed no changes in the range of influence in the area adjacent to the pressure plate. The displacement field was formed in the vicinity of the plate surface of 30mm away from the upper surface of the plate. There were certain differences in the range of influence of the displacement field formed by the particles. The 4×4 arrangement of the sample had a smaller range of influence than the influence range of the 3×3 samples, but the influence range of the displacement field was focused on the 0 to 30mm range and the 120 to 150mm range in the X direction and the 63 to 90mm range in the Y direction. However, depending on the arrangement of the aggregated stones, the influence range of the displacement field of the soil-rock aggregate was continuously reduced below the pressure plate.

When the stones were arranged in a 4×4 grid, the displacement field under the pressure plate had a maximum influence range of

25 to 90mm in the Y direction; when the stones were arranged in a 3×3 grid, the displacement field ranged from 9 to 90mm, which was the largest in the Y direction. The above data showed that the arrangement of the stone had a great influence on the range of the displacement field of the soil-rock aggregate, and the range of the displacement field gradually increased with the decrease in the number of stones and the intensity of the arrangement.

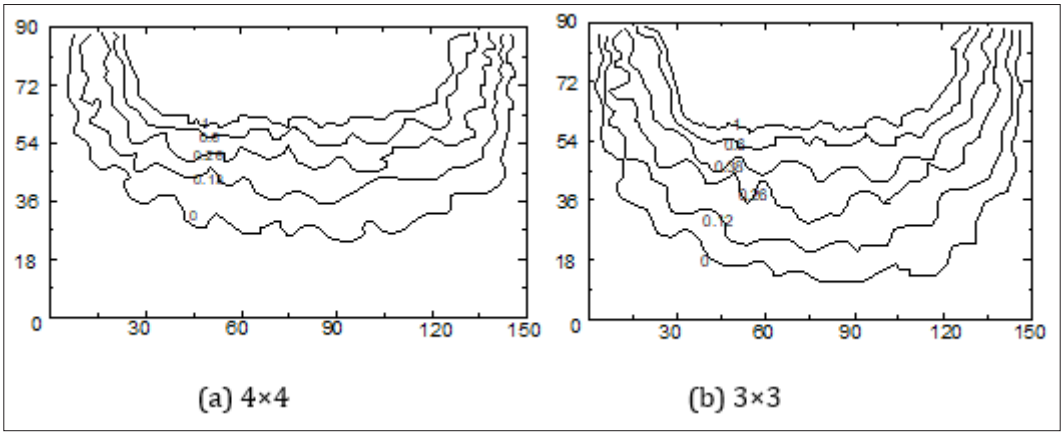

Figure 13: The displacement field of the soil-rock aggregate under two different types of stone arrangements.

Influences of loading rate on the soil-rock aggregate

In this test, the particle size of the soil particles was between 0.1 and 0.5mm, the stone arrangement was 4×4, and the loading rate was either 3mm/min and 5mm/min. The final displacement field distribution of the soil-rock aggregate at different loading rates is shown in Figure 14. It can be seen from Figure 14 that the displacement field profiles have the same pattern at different loading rates, and the displacement fields were formed near the plate surface 30mm from the upper surface of the plate. The formed of displacement fields were in the range between 0 to 30mm and 120 to 150mm in the X direction and 63 to 90mm in the Y direction. The displacement field below the pressure plate had an influence in the range of 18 to 90mm in the Y direction. Therefore, under the action of vertical force, the loading rate has little effect on the soil-rock aggregate.

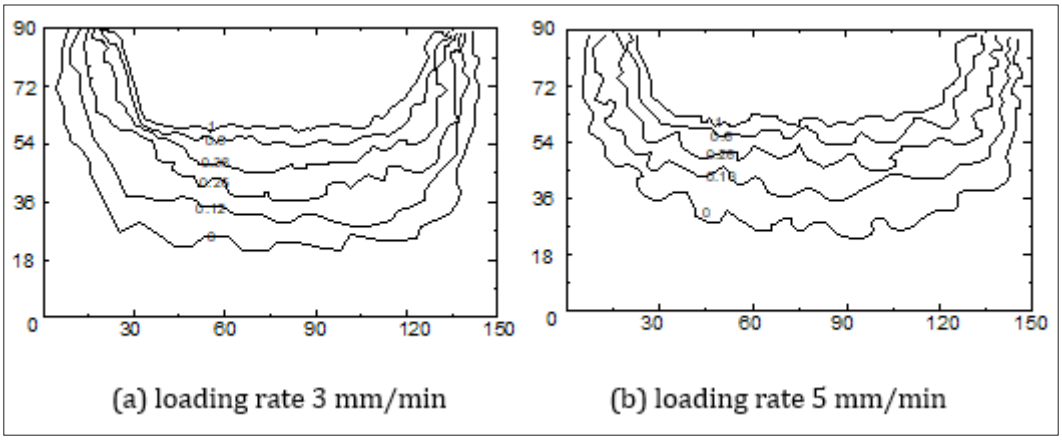

Figure 14: TThe displacement field of the soil-rock aggregate under different loading rates.

Conclusion

According to the similar model test principle, the transparent soil-rock aggregate model test system was established. The fully transparent-lateral confinement test mould was independently developed using transparent acrylic sheets. Then, we analyzed the influence of soil particle size, stone arrangement and loading rate on the deformation of an soil-rock aggregate by using the transparent-similar material uniaxial compression experiment system and combining the Photo-Infor image analysis and Post-Viewer post-processing software. The main research results were as follows:

A. According to the test results, the soil-rock aggregate was divided into the pressure plate influenced zone and the extended influenced zone. The migration of soil particles shifted with the movement of the pressure plate in the area affected by the pressure plate. With the movement of the pressure plate, the soil particles also shifted slowly. Until the end of the soil particle remodeling compaction, the pressure was transmitted downward. The soil particles were moved step by step until the loading was completed, and then, the particles showed gradation characteristics along the vertical downward direction.

B. The migration of the soil particles was divided into two parts in the influenced extended area. One was that the two sides of the soil particles below the pressure plate were pushed by the aggregated soil, so that the movement direction of the soil was less than 90° in the vertical direction. The angle decreased as the distance from the pressure plate increased. Second, the soil particles initially moved horizontally from the pressure plate in the extended area near the edge of the pressure plate. Then, as the pressure plate compression increased, the soil body moved upward, and the movement angle gradually increased.

C. Both the soil size and the arrangement of the stones have important influences on the displacement field of the soil-rock aggregate. With the increase in the particle size of the soil, the influence range of the displacement field gradually decreased. The soil-rock aggregate with particle sizes between 0.1 and 0.5mm had great influence on the displacement field. The smallest influence was from particles with sizes between 0.5 and 1.0mm. As the distribution density of the stone increased, the influence range of the displacement field of the soil-rock aggregate gradually decreased. In addition, the loading rate had less effect on the displacement field.

Acknowledgement

This research was funded by the National Natural Science Foundation of China (Grant Nos. 51804299, 51574222); the Natural Science Foundation of Jiangsu Province, China (Grant No. BK20180646).

References

1. Zevgolis IE (2018) Geotechnical characterization of mining rock waste dumps in central Evia, Greece. Environmental Earth Sciences 77: 566.
2. Chandler RJ (1973) The inclination of talus arctic talus terraces and other slopes composed of granular materials. Journal of Geology 81: 1-14
3. Deng YE, Yu J, Peng X (2014) Evolution characteristics of permeability and porosity of mudding weak permeability media with nonlinear flow. Applied Mechanics & Materials, pp. 580-583, 893-896.
4. Chang CS, Deng Y, Meidani M (2018) A multi-variable equation for relationship between limiting void ratios of uniform sands and morphological characteristics of their particles. Engineering Geology 237: 21-31.
5. Ng TT, Zhou W, Chang XL (2016) Effect of particle shape and fine content on the behavior of binary mixture. Journal of Engineering Mechanics 143: C4016008.
6. Huang M, Li Z (2006) Influences of particle size and interface energy on the stress concentration induced by the oblate spheroidal particle and the void nucleation mechanism. International Journal of Solids & Structures 43(14-15): 4097-4115.
7. Yin YZ, Wang YL (2014) Determine the shear strength of aeolian sand and bearing capacity. Applied Mechanics & Materials, pp. 580-583, 165-168.
8. Vieira CS, Lopes MDL, Caldeira L (2015) Sand-Nonwoven geotextile interfaces shear strength by direct shear and simple shear tests. Geomechanics & Engineering 5: 601-618.
9. Liu B, Ning Y (2011) Application of fractal theory to geotechnical engineering. Applied Mechanics & Materials 52-54: 1291-1295.
10. Qiang Y, Wang JC, Chen W (2013) An experimental study on the dynamic strength of soil-rock Aggregate. Applied Mechanics & Materials 353-356: 597-601.
11. Li Y, Zhang S, Zhang X (2018) Classification and fractal characteristics of coal rock fragments under uniaxial cyclic loading conditions. Arabian Journal of Geosciences 11: 201.
12. Wang Y, Li X, Li SD (2015) Cracking deformation characteristics for rock and soil aggregate under uniaxial compressive test. Chinese Journal of Rock Mechanics and Engineering 34: 3541-3552.
13. Sun HF, Ju Y, Xing MX (2014) 3D Identification and analysis of fracture and damage in soil-rock mixtures based on CT image processing. Journal of China Coal Society 39: 452-459.
14. Zhou B, Lu ZL, Wang HB (2013) Stress-strain relationship of soil-rock mixture based on homogenization theory. Geological Bulletin of China 32: 2001-2007.
15. Yuan WN, Li X, He JM (2013) Structure effect study of deformation and failure of rock and soil aggregate with CT technique. Chinese Journal of Rock Mechanics and Engineering 32: 3134-3140.